Energy 70 (2014) 110–120

Contents lists available at ScienceDirect

Energy

journal homepage: www.elsevier.com/locate/energy

A high efficiency oxyfuel internal combustion engine cycle with water direct injection for waste heat recovery

Zhi-Jun Wu*, Xiao Yu, Le-Zhong Fu, Jun Deng, Zong-Jie Hu, Li-Guang Li

School of Automotive Studies, Tongji University, Shanghai 200092, China

ARTICLE INFO

Article history:
Received 31 October 2013
Received in revised form
21 March 2014
Accepted 22 March 2014
Available online 21 April 2014

Keywords:
Oxyfuel combustion
Waste heat recovery
Water direct injection
IC engine
Engine efficiency

ABSTRACT

This paper presents a novel concept of combining water injection process with an oxyfuel internal combustion engine cycle to enhance thermal efficiency. Since the emission of NO_x is eliminated by using oxygen instead of air as oxidant, the exhaust gas is CO_2–water vapor mixture, and CO_2 is recovered through condensation of the exhaust gas at low cost. In this way, an ultra-low emission working cycle is achieved. The evaporation of injected water not only moderates the peak in-cylinder temperature, but also increases the mass of working gas inside the cylinder, therefore improves the thermal efficiency of the cycle. An ideal thermodynamic model combining an oxyfuel Otto cycle with water injection process was established to investigate the potential of the cycle thermal efficiency. Calculation results show that thermal efficiency reaches 53% when water injection temperature is 120 °C and 67% when water injection temperature reaches 200 °C. Moreover, bench tests were carried out on prototype engine based on this working cycle. Experimental results show that the thermal efficiency improves with the increase of both engine load and water injection mass, and indicated thermal efficiency increases from 32.1% to 41.5% under appropriate test condition.

1. Introduction

Carbon capture using oxyfuel combustion methods is considered to be one of the best ways to eliminate CO_2 emission [1]. In these methods, oxygen rather than air is utilized to combust the fuel with recycled carbon dioxide and/or water to limit combustion temperatures so leaving the products as mostly carbon dioxide and water vapor, as shown in chemical reaction equations (1) and (2).

$$\text{Traditional combustion}: \quad C_xH_y + O_2 + N_2 \rightarrow CO_2 + H_2O + NO + NO_2 + N_2 \tag{1}$$

$$\text{Oxyfuel combustion}: \quad C_xH_y + O_2 \rightarrow CO_2 + H_2O \tag{2}$$

The CO_2 not recycled can be captured after separated from exhaust gas through condensation process [2]. Economic evaluation of oxyfuel power plants has been taken out [3], and effect of boundary conditions on the performance of oxyfuel power plants is investigated, such as operating pressure [4], CO_2 cooling system [5], as well as flue gas recirculation [6]. Combustion characteristics of coal [7] as well as gases fuels [8] using oxyfuel combustion technique are also studied.

Clean Energy System Inc. used a direct heating steam turbine cycle which recycles only H_2O and is capable of achieving very high cycle efficiencies with power-plant costs lower than those for gas turbine combined cycle (GTCC) plants. High pressure recycled water was injected into the gas generator to produce a steam-rich mixture with carbon dioxide at high temperature and pressure [9]. Oxyfuel combustion power-plant cycles of this type have been called internal combustion Rankine cycles (ICRCs). Basic efficiencies for the ICRC steam turbine cycle of 65% or more are possible, and the overall efficiency is reduced to about 58%, considering the energy cost of separating oxygen from air, which is still a very high figure [10].

Reciprocating engine versions of the ICRC have been studied for the potential application in automobiles, and Fig. 1 shows the schematic of the ICRC system. Recycled water is preheated by engine coolant to around 100 °C and then heated up to even higher temperature by exhaust gas, and waste heat is converted to the internal energy of the recycled water. The water is then injected into the cylinder near top dead center to moderate the combustion process [11]. An ideal thermal efficiency of 56% was obtained, and higher thermal efficiency is possible with further optimization [12].

* Corresponding author.
E-mail address: zjwu@tongji.edu.cn (Z.-J. Wu).

http://dx.doi.org/10.1016/j.energy.2014.03.095
0360-5442/

Nomenclature

OF	Oxygen volume fraction (%)
p	Pressure (MPa)
W	Work (J)
T	Temperature (°C)
u	Specific internal energy (kJ/kg)
V	Volume (m^3)
c_v	Specific heat of constant-volume (kJ/kg K)
H	Enthalpy (J)
h	Specific enthalpy (kJ/kg)
p_{max}	Peak in-cylinder pressure (MPa)
Φ_{pmax}	Phase of peak in-cylinder pressure (° CA)
dp_{max}	Peak in-cylinder pressure rising rate (MPa/° CA)
Φ_{dpmax}	Phase of peak pressure rising rate (° CA)
W_i	Indicated work (J)
η_i	Indicated thermal efficiency (%)

Abbreviations

ICRC	Internal combustion Rankine cycle
ICE	Internal combustion engine
CI	Compression ignition
SI	Spark ignition
LHV	Lower heating value
IMEP	Indicated mean effective pressure
MEP	Mean effective pressure
ITE	Indicated thermal efficiency
A/F ratio	Air–fuel mass ratio
I/F ratio	Intake–fuel mass ratio
TDC	Top dead center
BDC	Bottom dead center
CA	Crank angle
NO_x	Nitrogen oxides
PM	Particulate matter

Water injection technique has been studied for many years to control NO_x emission in diesel engines. A co-injection system injecting stratified fuel-water spray in a traditional diesel engine has shown a notable effect on NO_x and PM emission [13]. Together with EGR, a heavy duty engine should be able to meet Euro V emissions levels [14]. Water injection is also used in SI engines to increase the working stability under higher compression ratio [15], and H_2 engine could also benefit from water injection in order to work under higher engine load [16]. But the mass of injected water is only 30–50% as much as the fuel delivery mass, and the cycle performance benefits little from the vaporization of injected water.

Recent study shows that water might also be a preferable working fluid to recover waste heat and generate torque directly to crankshaft in ICEs. Oak Ridge National Laboratory added a two-stroke heat recovery steam cycle to Otto cycle, and used partial exhaust event coupled with water injection to convert waste heat into usable work [17]. Calculation results show that the MEP (mean effective pressure) of the steam cycle can reach 2.5 bar. Fu et al. used waste heat to generate water vapor, and set-up a steam expansion cycle (open Rankine cycle) in one cylinder of a four-cylinder SI engine. Calculation results show that thermal efficiency is improved by 6.3% at engine speed of 6000 r/min [18]. However, the power density of the ICE based on these two cycles is decreased, since the steam cycles have much lower MEP value compared with SI or CI combustion cycles.

The ICRC engine merges the two ideas mentioned above together by direct injection of high temperature water during the combustion process. Because the reaction rate of the oxyfuel mixture is much faster than that of the air–fuel mixture, the injected water will have less negative impact on the combustion process, and converts the combustion heat to work output more effectively. Boretti et al. simulated a novel two-stroke CI engine burning hydrogen in oxygen in presence of large amounts of steam as residual gases. The water mass injected each cycle would be 10–

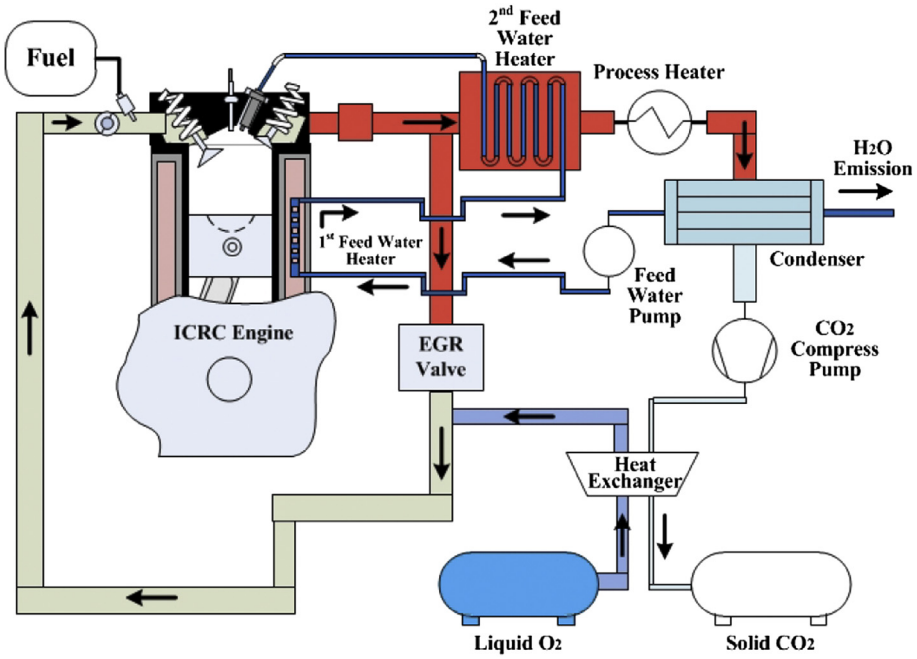

Fig. 1. Schematic of ICRC system.

50 times as much as H_2 mass injected in order to control the extremely high temperature. CFD modeling study shows that brake efficiency as high as 55% could be achieved [19]. This engine shares the similar idea as that of an ICRC engine, but little experimental study could be found in the literature.

In this paper, a thermodynamic model was established combining a traditional Otto cycle with water injection at top dead centre, and the effect of water injection temperature, water injection mass, as well as engine load on the thermal efficiency is studied. Furthermore, a self-designed prototype engine test bench was built, and the experimental results under different water injection mass and engine load are discussed.

2. Ideal thermodynamic analysis

Fig. 2 shows the in-cylinder pressure revolution with crank angle of a water injection cycle and a no water injection (dry) cycle. Assuming the compression and expansion process are adiabatic, and the water injection and evaporation process are instantaneous, Fig. 2 can be simplified to an Otto cycle combined with water injection process at TDC as shown in Fig. 3. Cycle 1–2–3–4–1 is a traditional Otto cycle. Water is injected at state point 3, where the combustion process has come to an end and the expansion stroke begins. The in-cylinder pressure will rise to state point 5 after water is injected, and the new combined working cycle changes to 1–2–5–6–1. According to the First Law of Thermodynamics for a control volume, the energy equation of any component process of this combined cycle could be written as.

$$Q_{in} - Q_{out} + W_{in} - W_{out} + m_{in}h_{in} - m_{out}h_{out} = \Delta E \tag{3}$$

In order to determine in-cylinder pressure and temperature after water injection, a computer program was written to solve the energy equation. The other traditional adiabatic process and constant-volume process were solved by STANJAN software of Reynolds [20] because specific heat change of working fluid under different temperature could be huge. The thermodynamic properties of in-cylinder components, such as O_2, CO_2, propane, and water vapor are listed in a built-in library file based on JANAF tables, and are called during calculation process.

2.1. Calculation formulas

The compression stroke of Otto cycle is assumed to be adiabatic, and the mass of working fluid is constant. Therefore, crankshaft work input would be the change of internal energy as in Eq. (4):

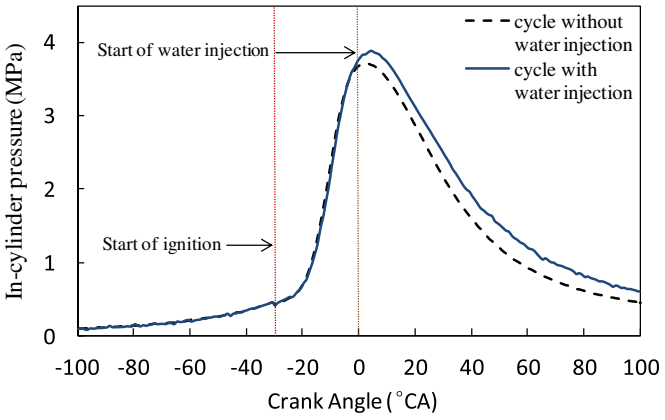

Fig. 2. In-cylinder pressure vs. crank angle of ICRC cycle.

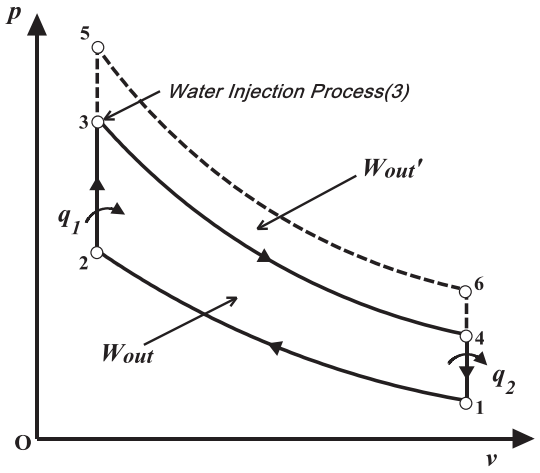

Fig. 3. Simplified P–V diagram of an ideal ICRC.

$$W_{1-2} = m_1(u_1 - u_2) \tag{4}$$

Combustion process starts at state point 2. After a constant-volume process, the in-cylinder pressure and temperature rises to state point 3 where water is injected. Assuming the evaporation process is instantaneous, Eq. (3) could be written as:

$$m_{water}h_{water} = m_5u_5 - m_3u_3 \tag{5}$$

$$m_5 = m_{water} + m_3,\ \ u_5 = c_{v5}T_5,\ \ u_3 = c_{v3}T_3 \tag{6}$$

where, h_{water} is the specific enthalpy of injected water. Together with ideal-gas law:

$$p_5V_3 = (n_w + n_3)R_mT_5,\ \ p_3V_3 = n_3R_mT_3 \tag{7}$$

where R_m is the mole gas constant, n_w is the moles of water injected, and n_3 is the total moles of in-cylinder working gas at state point 3. The thermodynamic state of state point 5 is uniquely determined, thus the temperature, pressure, and specific internal energy and enthalpy are fixed.

During experiments, water is injected under high pressure in order to speed up the vaporization process, as well as keep the water at liquid state under high injection temperature. The pump work of injected water must be considered. The definition equation of specific enthalpy is $h = u + pv$, and considering that the internal energy of injected water is gained from waste heat, the pump work of injected water per cycle could be given as

$$W_{pump} = m_{water}\left(p_{inj}v_{inj} - p_0v_0\right)\Big/\eta_{pump} \tag{8}$$

where W_{pump} represents the compression work consumed by the pump, p_{inj} and p_0 are the water injection pressure and ambient pressure, while v_{inj} and v_0 are the specific volume of water under injection pressure and ambient pressure. η_{pump} is the pump efficiency.

The expansion stroke is also supposed to be adiabatic, and the crankshaft work output is the change of internal energy shown in Eq. (9):

$$W_{5-6} = m_5(u_5 - u_6) \tag{9}$$

Therefore, work output, thermal efficiency and mean effective pressure (MEP) for each cycle would be

$$W_i = W_{5-6} + W_{1-2} - W_{\text{pump}} \tag{10}$$

$$\eta_i = W_i/q_1 = W_i \Big/ \left(m_{\text{fuel}} \times \text{LHV}_{\text{fuel}}\right) \tag{11}$$

$$\text{MEP} = W_i \Big/ V_{\text{disp}} \tag{12}$$

where m_{fuel} is the fuel consumption per cycle, LHV_{fuel} is the low heating value of fuel, and V_{disp} is the engine displacement. Moreover, partial pressure generated by water vapor is calculated by Dalton's Law of Partial Pressure, and specific volume and temperature of state points 5 and 6 are already known. Therefore, the expansion work produced by water vapor is calculated by Eq. (13):

$$W_{\text{vapor}} = m_{\text{water}}(u_{5\text{water}} - u_{6\text{water}}) - W_{\text{pump}} \tag{13}$$

where $u_{5\text{water}}$ and $u_{6\text{water}}$ are the specific internal energy of the in-cylinder working gas at state point 5 and state point 6.

2.2. Boundary conditions for calculation

As described above, there are a number of parameters to be set in order to calculate the thermal efficiency and work output of the combustion cycle. The initial conditions, assumptions, and constraints of this model are listed in Table 1, and engine geometry is listed in Table 2.

The initial temperature, intake composition, compression ratio, as well as water injection pressure are set according to experiments. Initial pressure is set from 0.3 to 1 bar, which covers the typical in-cylinder pressure at the end of the intake stroke under different engine load. Volume fraction of O_2 is set to 45% because CO_2 has strong side effects on flame propagation, and lower oxygen concentration will lead to instability of the combustion process, especially when water is injected. The water injection temperature is set from 0 °C to 200 °C to investigate the effect of injection temperature on cycle performances, and this is within the working temperature range of the commercial diesel injectors. In real engine applications, the water is supposed to be heated up by engine coolant and exhaust gas through heat exchangers before injected into the cylinder to recover the waste heat. The assumption of the instantaneous injection, vaporization, and mixing process are not physically realistic, but it is valid to estimate the upper bound on both the potential work output and thermal efficiency of this engine cycle. The in-cylinder temperature at 540 deg CA, where the expansion stroke ends at BDC, is set around 300 °C for two reasons. One is to keep the temperature of the water vapor above its dew point to prevent potential equipment damage due to droplet erosion and the resultant decrease in specific volume, the other is to keep the exhaust temperature high enough to heat up the recycled water.

Table 1
Initial conditions, assumptions, and constraints.

Initial conditions	
Initial temperature	20 °C
Intake composition	45% O_2, 55% CO_2
Compression ratio	9.2
Water injection pressure	20 MPa
Assumptions	
Initial pressure	0.03–0.1 MPa
Water injection temperature	0–200 °C
Water injection duration	Instantaneous at TDC
Water vaporization	Instantaneous at TDC
Water and working gas mixing	Instantaneous at TDC
η_{pump}	50%
Heat transfer to cylinder walls	None
Constraints	
Temperature at state point 4	≥300 °C

Table 2
Engine parameters.

Item	Content
IC engine type	Single cylinder SI engine
Bore (mm)	56.5
Stroke (mm)	49.5
Compression ratio	9.2
Displacement (cm^3)	124
Fuel type	C_3H_8
Cooling system	Air-cooled

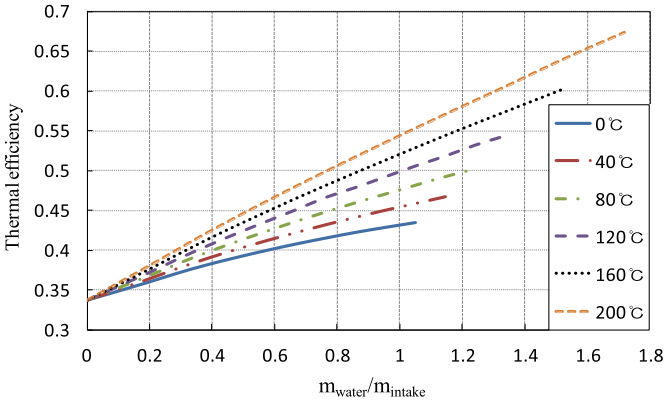

Fig. 4. Thermo efficiency under different injection temperature.

2.3. Effect of injection mass and temperature on cycle performances

The term intake–fuel (I/F) ratio is employed to replace the traditional air–fuel ratio because intake is a mixture of O_2/CO_2 instead of air, and it indicates the mass fraction between the intake charge and fuel delivery mass per cycle. The intake–fuel ratio in this section is set to 20 according to recent experiments, which is a lean-burn situation. The reason for this is because the test engine is air-cooled, and a richer mixture will lead to much higher in-cylinder temperature and causes damage to engine components and pressure transducer.

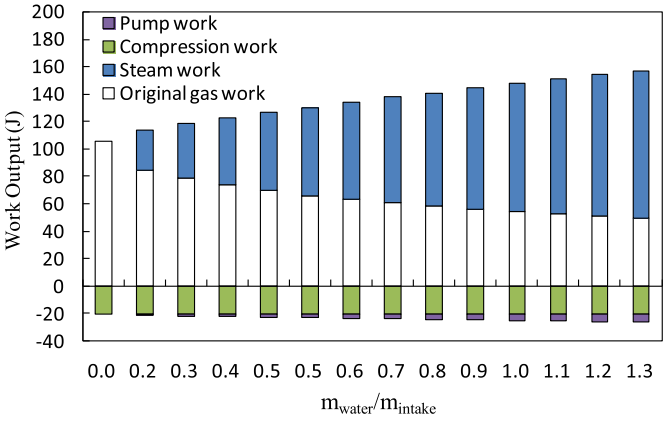

Fig. 5. Work ratio under different water injection mass.

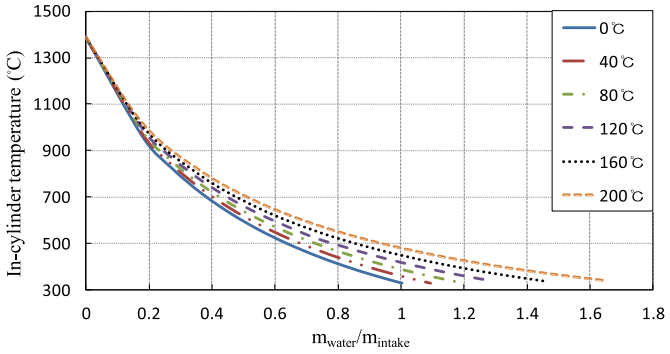

Fig. 6. Cylinder gas temperature at state point 4.

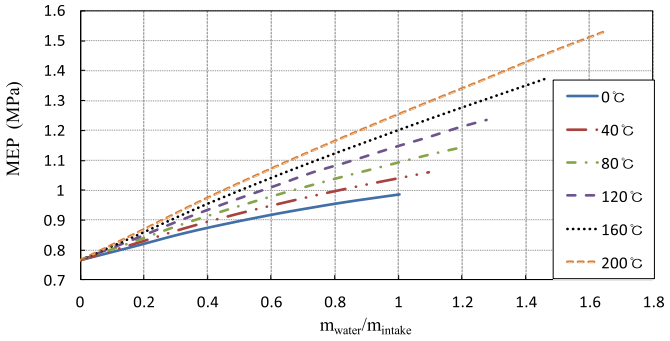

Fig. 8. MEP improvement with water injection.

Fig. 4 shows the relationship between thermal efficiency and water/intake ratio under different water injection temperature. The abscissa is the mass ratio between injected water and intake charge, and the calculation starts from m_{water}/m_{intake} equals 0, which is the dry cycle. It is clear that the thermal efficiency improves with the increase of water injection mass, and the slope of the thermal efficiency lines increases when injection temperature is higher.

Fig. 5 shows the relationship between the work generated by water vapor and original working gas, i.e. CO_2, residual O_2, and a small amount of water vapor as products of the combustion process, and the water injection temperature in this figure is 120 °C. It is obvious that the work produced by water vapor increases with the increase of the water injection mass, but the work output by original working gas is reduced because of the temperature drop caused by the added water. However, the total amount of work output increases under same fuel consumption, which means the thermal efficiency of the combined cycle is improved. It is seen from Fig. 5 that 75% of work output is produced by steam when m_{water}/m_{intake} reaches 1.3, and this is the reason that this combined cycle is referred to as a special kind of Rankine cycle.

Fig. 5 also shows the compression work and pump work calculated from Eq. (6). It is noted that the pump work of liquid water is much less than the compression work of the intake charge. This is because the specific volume of water is quite small compared with intake gas, and the change of specific volume of liquid under different pressure is negligible due to the incompressibility of water.

The injected water improves cycle performance in two ways. First, the injected water increases the mass of working gas inside the cylinder, and is capable of converting combustion heat into in-cylinder pressure more effectively and decrease the exhaust temperature. Fig. 6 shows the in-cylinder temperature at state point 6, which is the end of the working stroke. The temperature of a dry cycle is near 1400 °C (state point 4), which leads to extensive heat loss through exhaust gas, while the injected water can remarkably reduce the temperature of exhaust gas (as low as 300 °C).

Second, the injected water contains energy recovered from the waste heat, and the specific enthalpy of injected water is increased when water injection temperature is higher. According to Eq. (5), the in-cylinder pressure of state point 5 is increased, and the work produced by water vapor (area 3–5–6–4 in Fig. 3) is enhanced. Fig. 6 also indicates that the optimal water injection mass is increased under higher injection temperature, resulting in better cycle performance. Figs. 7 and 8 show that both vapor work and MEP of the cycle are increased under higher injection temperature. When injection temperature is 0 °C, the optimal improvement of MEP is 0.2 MPa and thermal efficiency increases from 33.7% to 43.4%. When injection temperature is 200 °C, MEP is increased from 0.68 MPa to 1.36 MPa and the thermal efficiency is improved from 33.7% to 67.3%.

2.4. Effect of engine load on cycle performances

In conventional SI engines, engine load is normally controlled by intake pressure, since the A/F ratio is fixed at stoichiometric ratio by the demand of three-way catalyst. As for oxyfuel combustion cycle, another way to adjust the engine load is to change the I/F ratio, because flame propagates stable within a wide range of I/F value when oxygen concentration is higher [21].

Figs. 9–12 show the cycle performance parameters under different I/F ratio. In-cylinder pressure at state point 1 is set to 0.5 bar, and water injection temperature is 120 °C for all cases. It is clear from Figs. 9 and 10 that higher MEP is achieved with lower thermal efficiency when more fuel is delivered, and this is because the higher heat loss due to the increase of exhaust gas temperature

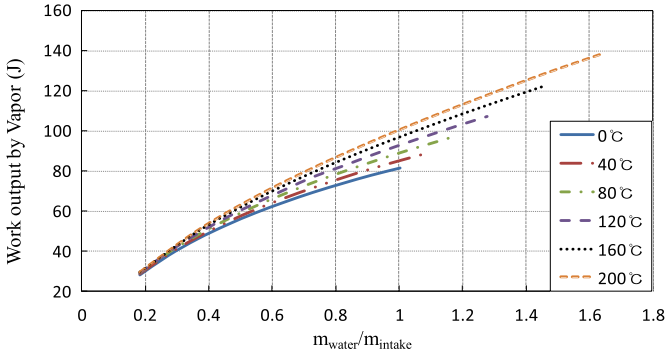

Fig. 7. Work output by water vapor.

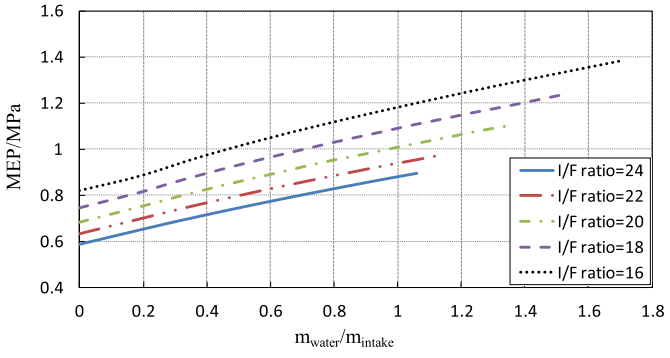

Fig. 9. MEP improvement under different I/F ratio.

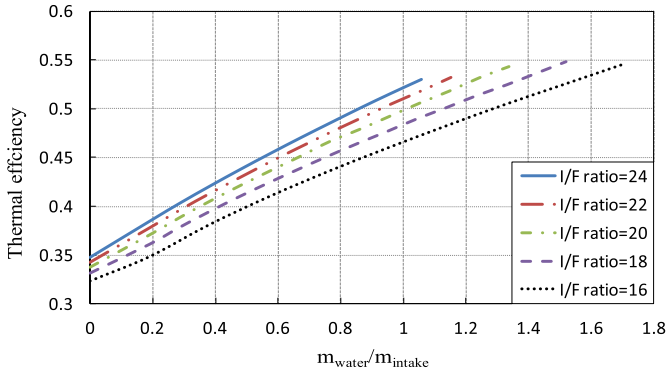

Fig. 10. Thermo efficiency under different *I*/*F* ratio.

shown in Fig. 11. This is practically the case for traditional IC engines when more torque or power is needed. The exhaust temperature is effectively controlled by injected water, and both MEP and thermal efficiency are improved, because the combustion heat is converted to work output more effectively by the added vapor. It is clear from Fig. 12 that the work generated by water vapor rises with the increase of in-cylinder temperature, but the thermal efficiency of *I*/*F* ratio = 16 case is the lowest under same water injection mass because of the higher fuel consumption. However, richer mixture also provides higher in-cylinder temperature which allows more water to be injected, and the interesting thing is that the optimal thermal efficiencies under different *I*/*F* ratio are basically the same.

Figs. 13–16 show the cycle performance parameters under different intake pressure. *I*/*F* ratio is set to 20, and the water injection temperature is 120 °C. Unlike the relationship shown in Fig. 11, the in-cylinder temperature evolutions of all four cases coincide with each other very well, as shown in Fig. 13. This is because the intake pressure does not affect the maximum in-cylinder temperature much. Thermal efficiency increases linearly with the increase of the water/intake ratio, and the optimal thermal efficiency stays around 54%, which is the same as the optimal thermal efficiency under different *I*/*F* ratio. The slope of MEP lines increase with the rise of intake pressure, because the work produced by water vapor is increased.

It is implied from the calculation results that water injection temperature is the most important factor to the performance of ICRCs. Higher injection temperature increases the maximum water injection mass, and increase the working gas inside the cylinder and enhance the cycle performance. Optimal thermal efficiency improves with the increase of water injection temperature, while the change of engine load does not affect the optimal thermal efficiency much.

3. Experimental results analysis

3.1. Experimental set-up and procedure

An overview of the experimental set-up is shown in Fig. 17. The engine was fueled with propane with the KN3-2B type electronic controlled gas nozzle (10) made by KN company in Japan. Oxygen and carbon dioxide gases were mixed at specific volume ratio and stored in tanks. The intake flow rate was regulated with flow controllers (13) and flow meters (14). A pressure multiplier (16) was designed to establish a stable injection pressure for the water injector, and the initial pressure was obtained from a compressed N_2 tank and amplified through the multiplier. Injection pressure was set around 20 MPa to minimize the fluctuation of injection rate caused by the variation of backpressure (in-cylinder pressure) during the injection process. The water injector is a solenoid common-rail diesel injector made by FAW Corporation, and the injected water was heated up in a self-designed heating device instead of the heat exchanger mentioned in Fig. 1 in order to conveniently investigate the effect of water injection process under specific injection temperature.

The engine was started with intake of air and then changed to oxyfuel combustion mode after synchronizing with the dynamometer. The engine ran for 5 min to bring it to a steady state before any measurements were carried out, and the engine speed is set to 2400 r/min for all cases. 100 cycles were collected for each condition including 50 continuous water injection cycles. The water injection cycles were distinguished from the other 50 dry cycles by water injection signals, and the indicator diagram and combustion parameters were drawn based on averaged cylinder pressure of the 50 wet cycles to study the combustion characteristics of each test condition. Water was injected at top dead centre, and the water temperature was 160 °C with injection duration of 0.3 ms and 0.4 ms. According to the calibration of the injector under this injection pressure, the water injection mass of the 0.3 ms and 0.4 ms cases is 45 mg and 60 mg per cycle.

3.2. Error analysis

The accuracy of the experiments has to be validated with an error analysis, since the errors in experiments can arise from calibration, environment, instrument conditions, as well as observations. Error analysis of the measured quantities can be accounted for in order to get the real measurement value, and the error analysis of the derived quantities such as indicated work and indicated thermal efficiency have to be estimated based on rout mean square method [22]. It gives the maximum error u of a function $f(x_1, x_2, \ldots x_n)$ as follows:

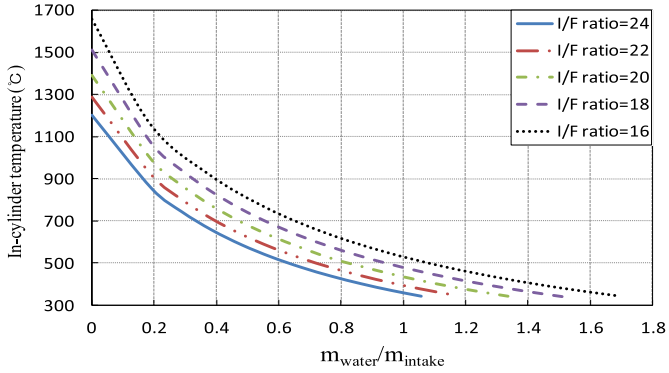

Fig. 11. Temperature of state point 4 under different *I*/*F* ratio.

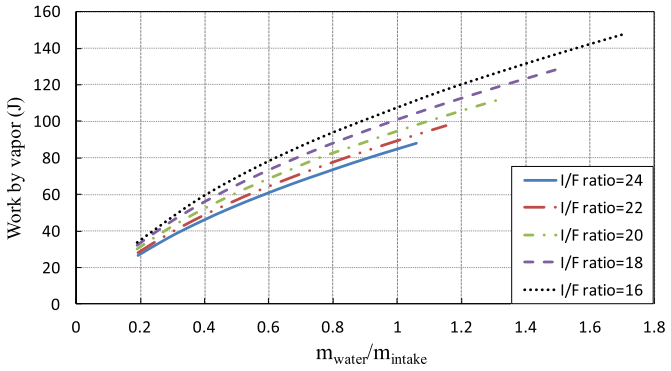

Fig. 12. Work generated by water vapor under different *I*/*F* ratio.

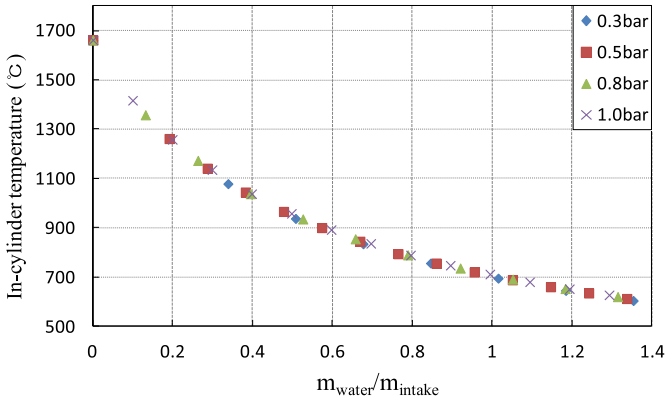

Fig. 13. Thermo efficiency under different intake pressure.

$$u(f(x_1x_2,\ldots x_n)) = \pm\sqrt{\sum_{i=1}^{n}\left(\frac{\partial f}{\partial x_i}\cdot u(x_i)\right)^2} \tag{14}$$

where u is the error limit of measured and derived quantities. The results are listed in Table 3 according to formula (14).

3.3. Effect of water injection mass on the cycle performances

The operating conditions and some of the combustion parameters are listed in Table 4. It is obvious that higher OF value will advance the combustion phasing, and the cycle performance is enhanced when the phasing of peak in-cylinder pressure is near TDC. Higher oxygen concentration leads to higher reaction rate, which will minimize the negative effects of water injection on the flame propagation process. It will also generate higher in-cylinder temperature and speed up the vaporization process of injected water, resulting in better indicated work and indicated thermal efficiency.

Fig. 18 shows cylinder pressure vs. cylinder volume under different injection duration of case 1. The peak in-cylinder pressure drops from 3 MPa to around 2.3 MPa after water is injected at TDC, which is in contradiction with the ideal cycle discussed in Section 2. But the in-cylinder pressure during the working stroke is still higher than that of the dry cycle, because the mass of working gas inside the cylinder is increased. The indicated thermal efficiency (ITE) of the water injection cycle increases from 31.6% to 35.3% when water injection duration is 0.3 ms, but drops to 34.8% when more water is injected.

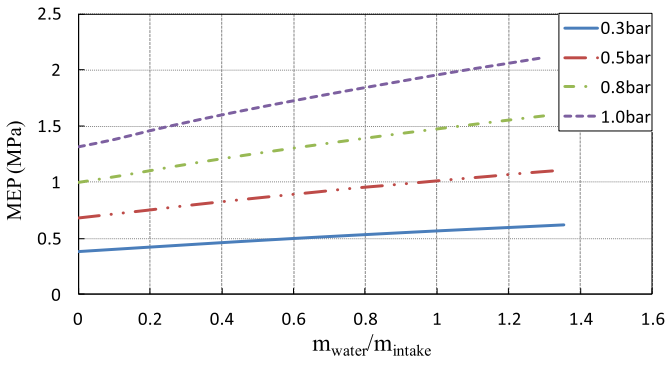

Fig. 14. MEP improvement under different intake pressure.

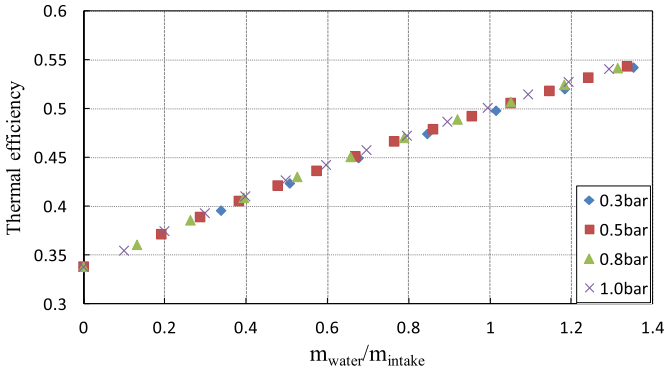

Fig. 15. Thermo efficiency under different intake pressure.

It is interesting to see in Fig. 19 that when OF value and fuel delivery mass is increased, the peak in-cylinder pressure of the "wet" cycle in case 2 increases notably. It is clear from Table 4 that the combustion retard of case 2 caused by water injection is less than that of case 1, and the ITE of the wet cycle increases from 35.2% to 38.2% when water injection mass is increased. The water injection cycle no longer suffers from the peak in-cylinder pressure drop shown in Fig. 18, and the in-cylinder pressure difference during expansion stroke caused by different water injection mass presents itself clearly.

Fig. 20 shows the P–V diagram of case 3 where oxygen concentration is 55% under same fuel delivery mass as in case 2. The peak in-cylinder pressure of the water injection cycle is increased by 7% compared with that of the dry cycle, and the ITE reaches 41.5% when water injection duration is 0.4 ms.

Fig. 21 shows the ideal ICRC under different water injection mass with same fuel delivery mass as case 3. The peak in-cylinder pressure of the calculation results is higher than the experimental results because of the assumption of adiabatic condition and constant-volume combustion process. Moreover, the peak in-cylinder pressure of water injection cycle increases when more water is injected according to calculation, but this phenomena is not observed through experiment. This is because the injection rate remains the same under same injection pressure, and the increase of injection duration does not affect the vapor mass inside the combustion chamber at the beginning of the injection process. Considering the engine speed of 2400 r/min, 1 ms of injection duration corresponds to 15 deg CA. Since water is injected at top dead center, which is 360 deg CA, the in-cylinder vapor mass of 0.4 ms case will exceed the 0.3 ms case after 365 deg CA. Although vapor mass is increased, but the volume of the combustion

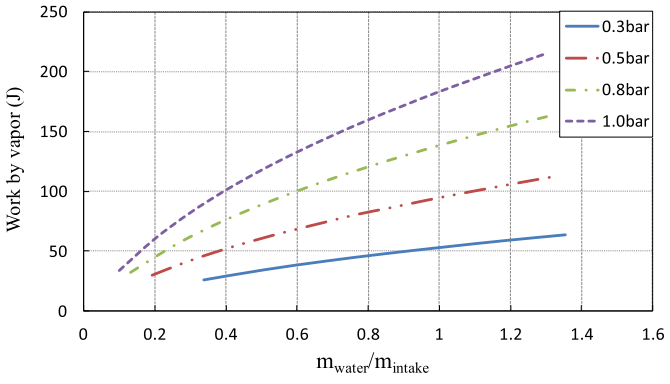

Fig. 16. Work generated by water vapor under different I/F ratio.

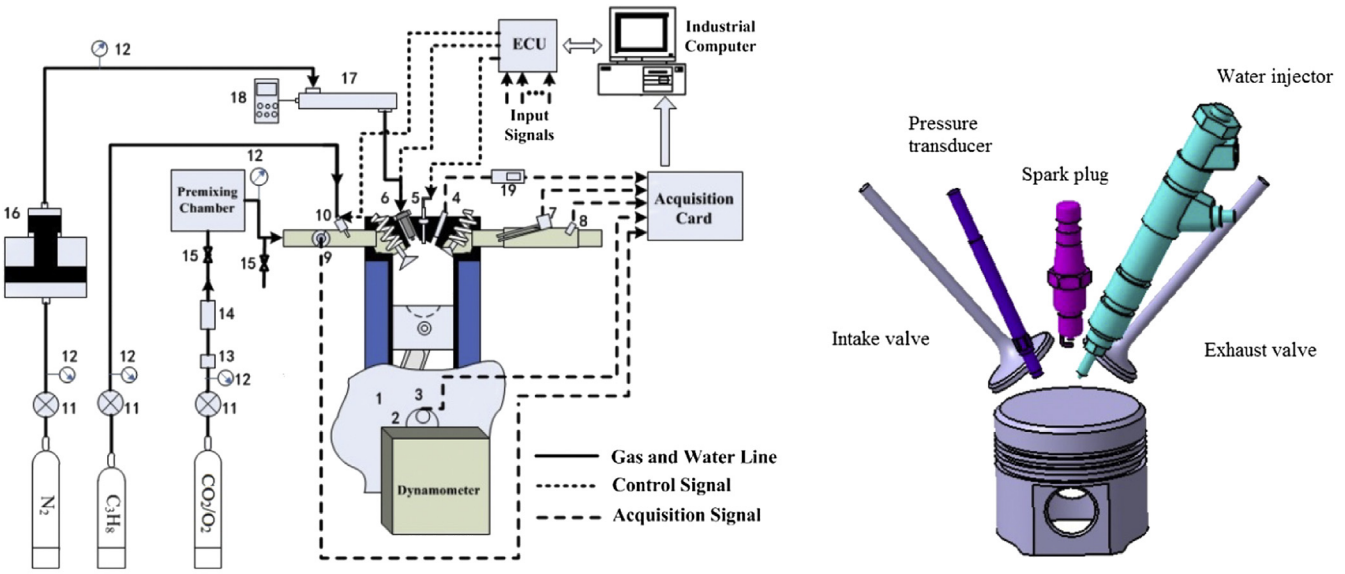

1 Engine; 2 Coupling; 3 Photoelectric encoder; 4 Pressure transducer; 5 Spark plug; 6 Water injector; 7 Emission analyzer; 8 Lambda sensor; 9 throttle; 10 Propane nozzle; 11 Pressure reduction valve; 12 Pressure gage; 13 Throttle valve; 14 Flowmeter; 15 Ball valve; 16 Pressure accumulator; 17 Water rail; 18 thermocouple; 19 charge amplifier

Fig. 17. Schematic of the test bench dedicated to ICRC engine and combustion chamber layout.

Table 3
Relative measurement error.

Instrument	Measuring range	Relative error (%)
Inlet gas pressure	0–0.2 MPa	±0.25
In-cylinder pressure	0–10 MPa	±0.5
O_2 concentration	0–50% vol	±1
Propane flow meter	0–25 L/min	±2.5
Crank angle encoder	–	±0.1
Engine speed	0–6000 r/min	±1
W_i	–	±0.5
η_i	–	±2.9

chamber also increases because the piston starts to move downwards, and the peak in-cylinder pressure of the two cases remains the same as each other. However, it is clear that the calculation results under different injection mass shares the same trend as the experimental results, which indicates the validity of the thermodynamic model, with the exception of case 1. The reason for this is that both the in-cylinder temperature and flame propagation process are seriously affected by water injection process when engine is running at lower load.

It is implied from above that the in-cylinder temperature plays an important role in the performance ICRC. The compression lines of water injection cycle and dry cycle in Fig. 18 do not match well with each other, and this is due to the fact that the water injection process affects the combustion process such that it causes the engine speed to vibrate. This will change the mass of intake charge under same throttling and valve timing. This difference is minimized when engine load is higher as shown in Figs. 19 and 20, which also indicates the improvement of working stability under higher engine load.

Fig. 22 shows the ITE from case 1 to case 3 and the modeling results calculated in Section 2.3. The efficiency trend of case 2 and case 3 under different injection mass is similar with the modeling results, and the experimental data get closer to the modeling results when in-cylinder temperature is higher. The modeling study set-up an upper bound of the efficiency of ICRC, and it is inferred from Fig. 22 that higher in-cylinder temperature will speed up the vaporization process, therefore lessen the gap between experimental results and thermodynamic analysis.

4. Discussion

The thermodynamic analysis in Section 2 assumes that both water injection process and evaporation process are instantaneous in order to investigate the upper bound of the thermal efficiency of

Table 4
Specifics of each test case.

Test condition		OF (%)	m_{fuel} (mg)	m_{water} (mg)	IMEP (MPa)	p_{max} (MPa)	Φ_{Pmax} (°CA)	dp_{max} (MPa/°CA)	Φ_{dpmax} (°CA)	W_i (J)	η_i (%)
Case 1	No water	45	4.2	0	0.54	3.0	368	0.16	358	67 ± 0.34	31.6 ± 0.9
	0.3 ms	45	4.2	45	0.60	2.33	378	0.12	365	74.7 ± 0.37	35.3 ± 1.0
	0.4 ms	45	4.2	60	0.59	2.29	379	0.08	366	73.7 ± 0.37	34.8 ± 1.0
Case 2	No water	50	4.9	0	0.62	3.47	366	0.20	354	77 ± 0.39	31.2 ± 0.9
	0.3 ms	50	4.9	45	0.70	3.40	372	0.16	360	87 ± 0.44	35.2 ± 1.0
	0.4 ms	50	4.9	60	0.76	3.43	373	0.15	359	94.3 ± 0.47	38.2 ± 1.1
Case 3	No water	55	4.9	0	0.64	3.62	363	0.23	350	79.4 ± 0.40	32.1 ± 0.9
	0.3 ms	55	4.9	45	0.75	3.87	367	0.21	354	92.8 ± 0.46	37.6 ± 1.1
	0.4 ms	55	4.9	60	0.83	3.87	369	0.20	355	102.4 ± 0.51	41.5 ± 1.2

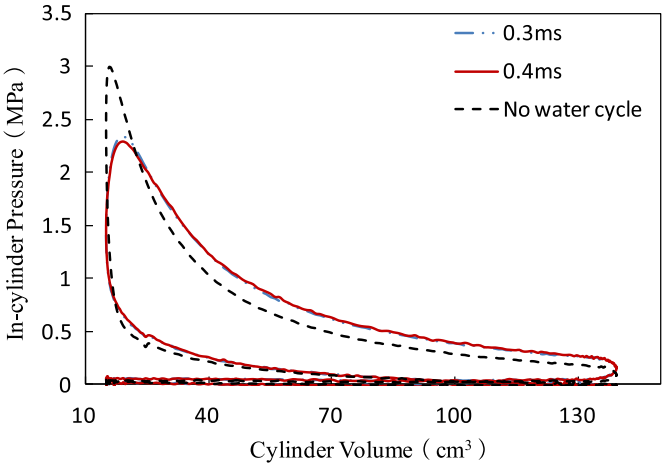

Fig. 18. *P–V* diagram under different injection duration of case 1.

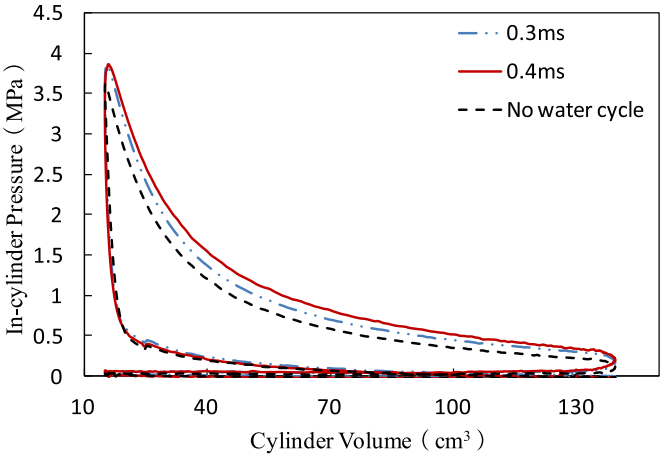

Fig. 20. *P–V* diagram under different injection duration of case 3.

ICRC, which supposes that the process a–d (or a–d′) shown in Fig. 23 is transient. Eq. (5) is established based on this assumption.

Because h_{water} is always positive when water temperature is above 0 °C, the in-cylinder pressure is always increased by the added water/vapor. However, the injected water at temperature T_a needs to be heated up to its saturation temperature T_b first. The injected water remains in liquid state from state point a to state point *b*, and the change of specific volume due to temperature change is negligible. Therefore, Eq. (3) changes into Eq. (15) at the beginning of the vaporization process (a–b).

$$m_{water}c_{vL}(T_a - T_b) = m_5u_5 - m_3u_3 \tag{15}$$

where c_{vL} is the specific heat value of liquid water. Since $T_b > T_a$, the left side of the equation is negative, which means the internal energy inside the combustion chamber is decreased, and the in-cylinder pressure will drop correspondingly. The actual cycle performance of the combustion cycle would be 1–2–7–6–1 instead of the ideal cycle 1–2–5–6–1 as shown in Fig. 24. Under even lower in-cylinder temperature, the time consumed from T_a to T_b is increased, and the combustion cycle will be 1–2–8–6–1, as shown in Fig. 18 where the engine load is the lowest of the three test cases.

It is implied from above that both the injection temperature and in-cylinder temperature are crucial to improve the cycle performance of the ICRC. Higher injection temperature not only recovers more energy from the waste heat, but also narrows the temperature difference between the injection temperature and local critical temperature of the injected water. It is clear from Fig. 23 that if the temperature of injected water is T_a' instead of T_a, the heating process of liquid water will be shortened, hence, a better cycle performance is expected.

Thermodynamically, higher in-cylinder temperature is capable of increasing the internal energy of the water vapor, for example from state point d to state point d′. Since the outlet temperature remains the same at state point 6, the total amount of expansion work generated by water vapor will increase. But the accompanying fuel consumption increase will cause the thermal efficiency to fall. When it comes to experiments, the in-cylinder temperature can be increased by higher oxygen concentration or advanced combustion phasing, and higher in-cylinder temperature will provide higher heat transfer rate from the working gas to water mist. Therefore, the vaporization process can be shortened, and the penalty of peak in-cylinder pressure drop is reduced.

Since O_2 is separated from the air, it is necessary to estimate the energy cost of O_2 separation, in order to get the overall efficiency of ICRC. Mass production of high purity oxygen utilizing the latest oxygen generation technology available enables the power consumption to be reduced to as low as 0.21 kWh/kg [23], which is

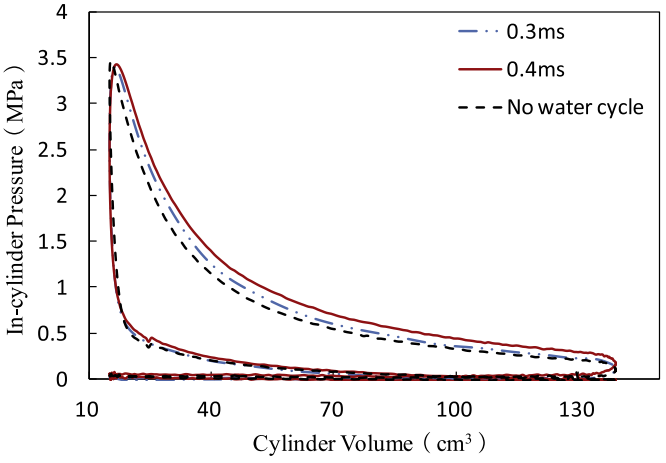

Fig. 19. *P–V* diagram under different injection duration of case 2.

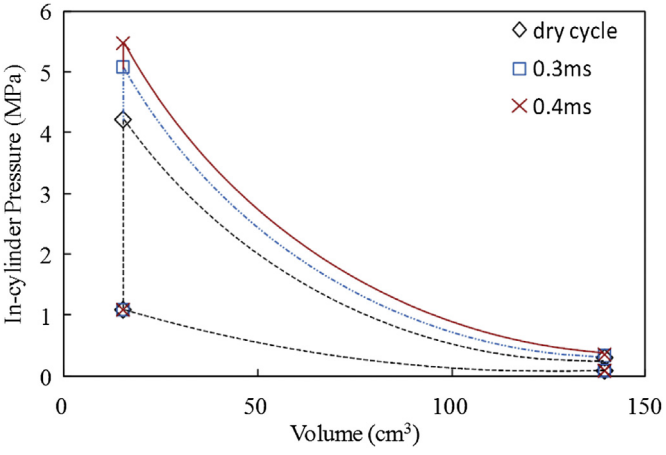

Fig. 21. Calculation results under same parameters as in case 3.

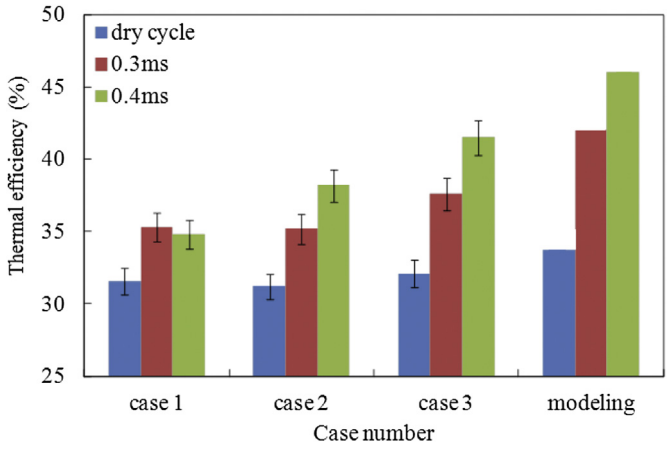

Fig. 22. Thermo efficiency under different engine load.

0.756 J/mg. Therefore, the efficiency cost of O_2 separation can be calculated according to Eq. (16):

$$\eta_{O_2} = m_{O_2} \times 0.756 \Big/ \left(m_{\text{fuel}} \times \text{LHV}_{\text{fuel}}\right) \tag{16}$$

where m_{O_2} is the oxygen mass burnt per cycle, m_{fuel} is the fuel consumption per cycle, LHV_{fuel} is the low heating value of fuel.

According to the equation of propane combust with oxygen:

$$C_3H_8 + 5O_2 = 3CO_2 + 4H_2O \tag{17}$$

The oxygen mass need per cycle will be 3.63 times higher than the fuel delivery mass, therefore, it can be estimated that the efficiency cost by oxygen separation will be 5.4%, which means that thermal efficiency of ICRC should be higher than 45% in order to keep up with the efficiency of diesel engines. It is noted this analysis is made according to an SI engine with compression ratio of 9.2. In the future, a CI version of ICRC engine might be available, and the thermal efficiency improvement will be much higher.

Overall, this novel combustion cycle has the potential of achieving an ultra-low emission with high thermal efficiency and high power density using fossil fuels. Although the original idea of this type of engine is for automotive application, it may be more suitable for power generation in industries and commercial buildings, where an air separation plant could be built, and cost of O_2 would be negligible.

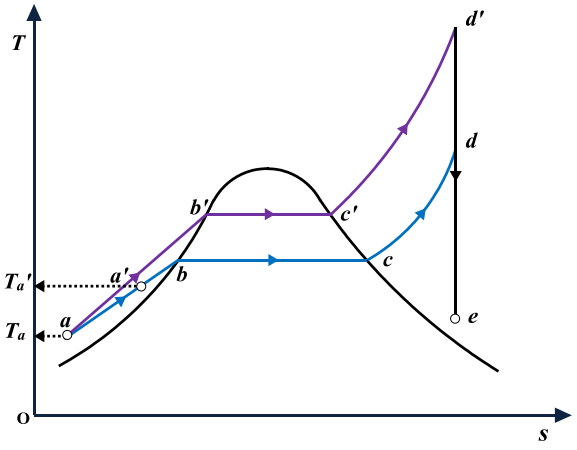

Fig. 23. *T–S* diagram of water and steam.

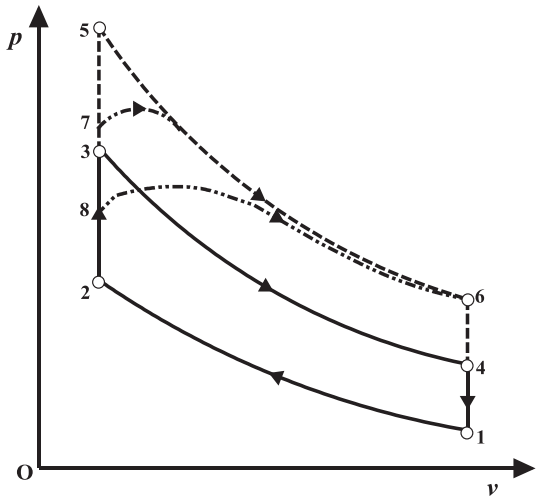

Fig. 24. Ideal *P–V* diagram considering evaporation process.

5. Conclusion

One of the reasons for CI engine having higher thermal efficiency than SI engine is that SI engine suffered from higher exhaust temperature due to lower compression ratio and fixed stoichiometric air–fuel mixture. The novel combustion cycle presented in this paper utilizes water direct injection to increase working gas near TDC, and converts the combustion heat into work more effectively. Moreover, water is heated up through engine coolant and exhaust gas before injected into the cylinder. Waste heat is recovered to produce work and transmits directly to the crankshaft, and higher thermal efficiency is expected. An ideal thermodynamic cycle was established to investigate the upper bond of the performance of this cycle, and the calculation results are compared with the experimental data, and the conclusions are given as follows

1) The cycle performance increases significantly by the added water. Modeling results show that water injection process can control the exhaust temperature, and both thermal efficiency and MEP are improved with the increase of injection mass and injection temperature. The Optimal thermal efficiency increases from 33% to 53% when water injection temperature is 120 °C and to 67% when water injection temperature reaches 200 °C. The optimal MEP increment under these two injection temperatures is 0.4 MP and 0.68 MP.
2) Higher in-cylinder temperature provided by higher engine load will lead to higher vapor temperature, and improves the working capacity of the water vapor, and improves the MEP. However, the optimal thermal efficiency remains the same under different engine load due to the fact that fuel consumption is also increased under higher engine loads.
3) Experimental results indicate that the in-cylinder temperature is crucial to improve cycle performance. Higher in-cylinder temperature will shorten the vaporization process and lessen the performance gap between the theoretical and practical combustion cycle. Indicated thermal efficiency is increased from 32.1% to 41.5% under appropriate test condition, and IMEP improvement of 0.2 MPa is achieved.

References

[1] Buhre BJP, Elliot LK, Sheng CD, Gupta RP, Wall TF. Oxy-fuel combustion technology for coal-fired power generation. Prog Energy Combust Sci 2005;31:283–307.

[2] Metz B, Davidson O, deConinck HC, Loos M, Meyer LA. IPCC special report on carbon dioxide capture and storage. Cambridge, UK: Cambridge University Press; 2005. http://www.ipcc.ch/pdf/special-reports/srccs/srccs_wholereport.pdf.
[3] Pak Pyong Sik, Lee Young Duk, Ahn Kook Young. Characteristics and economic evaluation of a power plant applying oxy-fuel combustion to increase power output and decrease CO_2 emission. Energy 2010;35:3230–8.
[4] Hong Jongsup, Field Randall, Gazzino Narco, Ghoniem Ahmed F. Operating pressure dependence of the pressurized oxy-fuel combustion power cycle. Energy 2010;35:5391–9.
[5] Fiaschi Daniele, Manfrida Giampaolo, Mathieu Philippe, Tempesti Duccio. Performance of an oxy-fuel combustion CO_2 power cycle including blade cooling. Energy 2009;34:2240–7.
[6] Granados DA, Chejne Farid, Mejia Juan M, Gomez CA, Berrio A, Jurado WJ. Effect of flue gas recirculation during oxy-fuel combustion in a rotary bement kiln. Energy 2014;64:615–25.
[7] Zebian Hussam, Mitsos Alexander. Pressurized oxy-coal combustion: ideally flexible to uncertainties. Energy 2013;57:513–26.
[8] Andersson K, Johnsson F. Flame and radiation characteristics of gas-fired O_2/CO_2 combustion. Fuel 2007;86:656–68.
[9] Marin O, Bourhis Y, Perrin N, Di Zanno P, Viteri F, Anderson R. High efficiency zero emission power generation based on a high temperature steam cycle. In: 28th International technical conference on coal utilization and fuel systems, Clearwater, FL; 2003.
[10] Bilger RW. Zero release combustion technologies and the oxygen economy. In: Fifth international conference on technologies and combustion for a clean environment, Lisbon, Portugal; 1999. pp. 1039–46.
[11] Bilger RW, Wu Zhijun. Carbon capture for automobiles using internal combustion rankine cycle engines. J Eng Gas Turb Power 2009;131:034502.
[12] Wu Zhijun, Yu Xiao. CO_2 capture automotive engine system based on internal combustion ranking cycle. J Jilin Univ 2010;40:1199–202.
[13] Kohketsu S, Mori K, Sakai K, Nakagawa H. Reduction of exhaust emissions with new water injection system in a diesel engine; 1996. SAE Paper No. 960033.
[14] Stanglmaier Rudolf H, Dingle Philip J, Stewart Daniel W. Cycle-controlled water injection for steady-state and transient emissions reduction from a heavy-duty diesel engine. J Eng Gas Turb Power 2008;130:032801.
[15] Lanzafame R. Water injection effects in a single-cylinder CFR engine; 1999. SAE Paper No.1999-01-0568.
[16] Nande A, Wallner T, Naber J. Influence of water injection on performance and emissions of a direct-injection hydrogen research engine; 2008. SAE Paper No. 2008-01-2377.
[17] Conklin James C, Szybist James P. A highly efficient six-stroke internal combustion engine cycle with water injection for in-cylinder exhaust heat recovery. Energy 2010;35:1658–64.
[18] Fu Jianqin, Liu Jingping, Ren Chengqin, Wang Linjun, Deng Banglin, Xu Zhengxin. An open steam power cycle used for IC engine exhaust gas energy recovery. Energy 2012;44:544–54.
[19] Boretti Alberto, Osman Azmi, Aris Ishak. Direct injection of hydrogen, oxygen and water in a novel two stroke engine. Int J Hydrogen Energy 2011;36:10100–6.
[20] Reynolds WC. STANJAN chemical equilibrium solver, version 3.94. Stanford, CA: Department of Mechanical Engineering, Stanford University; 1987.
[21] Yu Xiao, Wu Zhijun. Simulation on effect of EGR on oxy-fuel IC engine. Appl Mech Mater 2012;130:790–5.
[22] Sahin Z, Durgun O, Bayram C. Experimental investigation of gasoline fumigation in a single cylinder direct injection (DI) diesel engine. Energy 2008;33:1298–310.
[23] Osman Azmi. Feasibility study of a novel combustion cycle involving oxygen and water; 2009. SAE paper no. 2009-01-2808.